Room-temperature ionic liquid assisted fabrication of sensitive electrochemical immunosensor based on ordered macroporous gold film

Xiaojun Chen,[ab] Jinjun Zhou,[a] Jie Xuan,[a] Wei Yan,[a] Li-Ping Jiang[a] and Jun-Jie Zhu*[a]

Received 25th April 2010, Accepted 24th June 2010
DOI: 10.1039/c0an00264j

A novel label-free highly sensitive electrochemical impedance spectroscopy (EIS) immunosensor was fabricated based on the highly ordered macroporous gold film (HOMGF) in the presence of room-temperature ionic liquid (IL) for the detection of human Apolipoprotein B-100 (ApoB-100). The antibody of ApoB-100 (Ab) was adsorbed directly onto the HOMGF electrode surface and maintained its bioactivity. After the residual active sites at the electrode were passivated by BSA, the mixture of $BMIm^+BF_4^-$ and silica sol was dropped onto the electrode to entrap the adsorbed Ab and BSA molecules firmly. The addition of IL could prevent the inactivation of Ab by releasing alcohol during the sol–gel process, and the conductivity of the IL-gel membrane was increased. Of particular interest is the fact that the fabricated immunosensor could be used at 60 °C. This could be attributed to the interconnected porosity of the IL-gel membrane, which can prevent Ab from unfolding and losing its bioactivities. The immunosensor also exhibited a highly sensitive response to ApoB-100 with the lowest concentration of 5 fg mL^{-1}. The detection of ApoB-100 levels in five sera samples obtained from hospital showed acceptable accuracy with that using commercial immunonephelometry method.

1. Introduction

The development of the methodology for probing disease markers at a low detection limit is a great challenge. Coronary artery disease (CAD) is one of the leading causes of mortality all of the world.[1] Studies indicated that cholesterol-enriched low density lipoproteins (LDL) in plasma could promote the deposition of plasma lipids in the artery wall and thereby elicit the formation of fatty streaks and/or atherosclerotic plaques.[2] The structure of LDL contains a hydrophobic core of cholesteryl surrounded by a polar coat composed primarily of phospholipids and a 513 kDa protein called apolipoprotein B-100 (ApoB-100). ApoB-100, the only protein on LDL, has become a good disease marker of CAD,[3] and it is very important to develop a sensitive method for the detection of ApoB-100. Although immunonephelometry has now been widely used in clinic for the detection of ApoB-100, the sensitivity is relatively poor.[4] Some other sensitive methods, involving radioimmunoassay (RIA)[5] and enzyme linked immunosorbent assay (ELISA),[6] may be inconvenient because of sophisticated instrumentation and time-consuming steps. Therefore, searching for simple, sensitive, reliable, and inexpensive diagnostic methods for ApoB-100 is of considerable interest. Electrochemical immunoassay with the features of low cost as well as high sensitivity are now used frequently in the clinical determinations of disease markers[7–9] and two kinds of sensitive electrochemical immunosensors for the direct determination of LDL was developed.[10,11] Among electrochemical immunoassays, electrochemical impedance spectroscopy (EIS) has been paid a lot of attention because it is a sensitive label-free technique with quite simple operation. The antigen-antibody (Ag-Ab) recognition can be reflected directly by the change of electrical impedance signals.[12]

The most important thing in developing immunosensors is to effectively immobilize biomolecules on the electrode surface in their native status,[13] and a variety of strategies have been introduced. Biomolecules can be immobilized through physical adsorption,[14,15] covalent bond,[16,17] self-assembly,[18–20] Langmuir–Blodgett deposition[21,22] and entrapment within a membrane of polymer[23–25] or sol–gel.[26,27] Among these immobilization methods, the sol–gel immobilization process is widely used due to its convenient preparation, tunable porosity, transparency, chemical stability and high loading of biomolecules. Biomolecules entrapped in sol–gel membranes usually exhibit better activity and stability than free ones.[28–30] However, there are some drawbacks in the sol–gel immobilization process. One is the shrinkage of gel membrane in the condensation and drying process which may cause the leakage of biomolecules. The released alcohols during the hydrolysis of silicon alkoxide can inactivate the entrapped biomolecules. The slow rate of substrate diffusion or electron transfer in silica matrices can decrease the biosensor sensitivity. To overcome these drawbacks, some additives such as sugars, amino acids, polyols and surfactants are used to stabilize biomolecules in sol–gel matrices. The additives can increase activity and stability of immobilized biomolecules by altering hydration of biomolecules. They can also improve gel properties by participating in condensation reactions with free alcohol precursors and reducing shrinkage *via* a "pore filling" effect.[31–33]

Room temperature ionic liquids (ILs) are composed entirely of ions at ambient temperature. They have been widely used as green solvents because of their unique physicochemical properties, such as high thermal stability, negligible vapor pressure,

[a]*Key Lab of Analytical Chemistry for Life Science (MOE), School of Chemistry and Chemical Engineering, Nanjing University, Nanjing, 210093, P. R. China. E-mail: jjzhu@nju.edu.cn; Fax: +86-25-83317761; Tel: +86-25-83594976*
[b]*College of Sciences, Nanjing University of Technology, Nanjing, 210009, P. R. China*

good electrochemical stability and conductivity.[34] Recently, ILs were used as a new kind of additive in silica gel matrix since the biomolecules encapsulated in the IL-gel matrix showed enhanced activity and stability.[35] Lee *et al.* reported the hydrolysis and esterification activities of lipase co-immobilized in IL-gel were 10-fold and 14-fold greater than in pure silica gel.[36] Zhao *et al.* studied the direct electrochemistry of hemoglobin (Hb) adsorbed on the surface of sol/IL/Nafion modified electrode, and the Hb exhibited an obvious electrocatalytic activity for the reduction of oxygen with the detection limit of 3.2 nM.[37] Recently, ionic liquid doped polyaniline inverse opals were used to fabricate an electrochemical immunoassay for the determination of hepatitis B surface antigen.[38]

Herein, a novel label-free EIS immunosensor for the detection of human ApoB-100 was fabricated by combining IL-gel complex membrane with HOMGF modified electrode. The concentration of ApoB-100 was measured with EIS by the corresponding specific interaction between ApoB-100 and Ab. The increased electron-transfer resistance (R_{et}) values were proportional to the logarithmic value of ApoB-100 concentrations in the linear range of 5 fg mL^{-1} to 50.0 pg mL^{-1}. The high sensitivity could be ascribed to the large active surface of HOMGF, the good conductivity of IL-gel matrix and the poor conductivity of ApoB-100. The immunosensor also presented excellent thermostability at 60 °C, which was due to the reduced deactivation of the immobilized Ab molecules in the confined space of IL-gel host matrix during the thermal treatment process.

2. Experimental

2.1 Chemicals and materials

Human ApoB-100 standards (0.5, 1.0, 1.5, 2.0 mg mL^{-1}) with the isoelectric point of 6.58 and 12.0 mg mL^{-1} polyclonal Ab were purchased from Zhejiang Elikan Biological technology Co. Ltd. Human prealbumin (PAB) was obtained from Xiamen Yutaikang Imports and Exports Biological Co. The monodispersed silica spheres with the diameters of 0.25, 0.5 and 1.0 μm were obtained from Alfa Asear. Human serum samples were obtained from Affiliated Drum Tower Hospital of Nanjing University Medical School and used as received. $BMIm^+BF_4^-$ (1-butyl-3-methylimidazolium tetrafluoroborate) and $BMIm^+PF_6^-$ (1-butyl-3-methylimidazolium hexafluorophosphate) (purity > 99%) were purchased from Lanzhou Institute of Chemical Physics, Chinese Academy of Sciences and were dried in vacuum at 60 °C for 24 h before use, stored in a desiccator as well. Tetraethyl orthosilicate (TEOS) was obtained from Shanghai Sinopharm Chemical Reagent Co. Ltd. (SCRC) (≥99%). Bovine serum albumin (BSA, 96–99%) was obtained from Sigma (St. Louis, MO). Phosphate-buffered saline (PBS, 50 mM, pH 7.0) were prepared by varying the ratio of NaH_2PO_4 and Na_2HPO_4. The standard ApoB-100 solutions were prepared daily in the PBS, and the Ab was stored at 4 °C. All other chemicals, such as anhydrous ethanol (EtOH), acetone, H_2SO_4, H_2O_2, NaOH, and $HAuCl_4 \cdot 4H_2O$ were of analytical grade and were used without further purification. Ultrapure fresh water obtained from a Millipore water purification system (MilliQ, specific resistivity > 18MΩ cm^{-1}, S. A. Molsheim, France) was used in all runs.

2.2 Apparatus

The electrochemical impedance measurements were carried out with an Autolab PGSTAT12 (Eco chemie, BV, The Netherlands) and controlled by GPES 4.9 and FRA 4.9 softwares. Cyclic voltammetric measurements were performed on a CHI660B electrochemical workstation (Shanghai CH Instruments Co.). A conventional three-electrode system was used comprising a platinum foil as the auxiliary electrode, a saturated calomel electrode (SCE) as the reference and a HOMGF modified electrode as the working electrode. All potentials herein are reference to the SCE. The geometric area of the working electrode was controlled by insulating tape covering the edges of SiO_2 layers and determined to be 0.07 cm^2. The IL-gel matrix was calcinated by a programmed temperature muffle furnace (Switzland, NEY6-1350A). The morphology of the matrix after the removal of the IL was characterized by transmission electron microscopy (TEM, JEOLJEM-2100). The sample for TEM was prepared by dropping a diluted suspension of silica powder onto a standard carbon-coated (20–30 nm) formvar film on a copper grid (230 mesh). Nitrogen adsorption and desorption isotherms were measured at −196 °C with a Micromeritics ASAP 2020 analyzer. The specific surface area was determined using the standard Brunauer–Emmett–Teller (BET) method, while the pore size distribution was calculated by the Barrett–Joyner–Halenda (BJH) method. The morphology of the HOMGF modified electrode was verified by field-emission scanning electron microscopy (FESEM, HITACHI S4800).

2.3 Fabrication of the ApoB-100 immunosensor

The fabrication process of the immunosensor is shown in Scheme 1. Preparation of the HOMGF modified gold electrode was described in our previous paper.[39] A clean gold substrate was immersed vertically into a diluted SiO_2 suspension (Scheme 1a), which was prepared by ultrasonic dispersing 0.35 g SiO_2 spheres into a 60 mL water–ethanol mixture (10/90 v/v). A temperature-controlled vibration-free furnace chamber was used to keep the temperature at 35 °C. Two days later, a three-dimensional silica close-packed colloidal crystal formed through solvent evaporation (Scheme 1b). After that, the silica crystal template was sintered at 250 °C to ensure its mechanical strength. The electrode area was controlled by an apertured insulating tape covering the edge of SiO_2 layers and was determined to be 0.07 cm^2 (Scheme 1c). Gold nanoparticles were electrochemically deposited into the template interspaces at a potential of 0.55 V (Scheme 1d). The SiO_2 spheres could be removed by 5% HF, As a result, a HOMGF modified gold electrode was obtained (Scheme 1e).

The IL-sol was synthesized by mixing ethanol (6 mL), TEOS (6 mL) and IL (0.5 mL) with a magnetic stirrer. 200 μL of 5 mM NaOH and 1.2 mL of H_2O were added drop by drop during stirring. Finally, the total system was refluxed at 60 °C for 30 min until a clear, homogeneous sol formed.

The obtained HOMGF modified gold electrode was immersed into a 500 μg mL^{-1} Ab solution overnight at 4 °C (Scheme 1f), and 3% (w/w) BSA solution was used to block the active sites of the electrode. Then, 6 μL prepared IL-sol was dropped onto the electrode and dried for 12 h at 4 °C, immobilizing the adsorbed

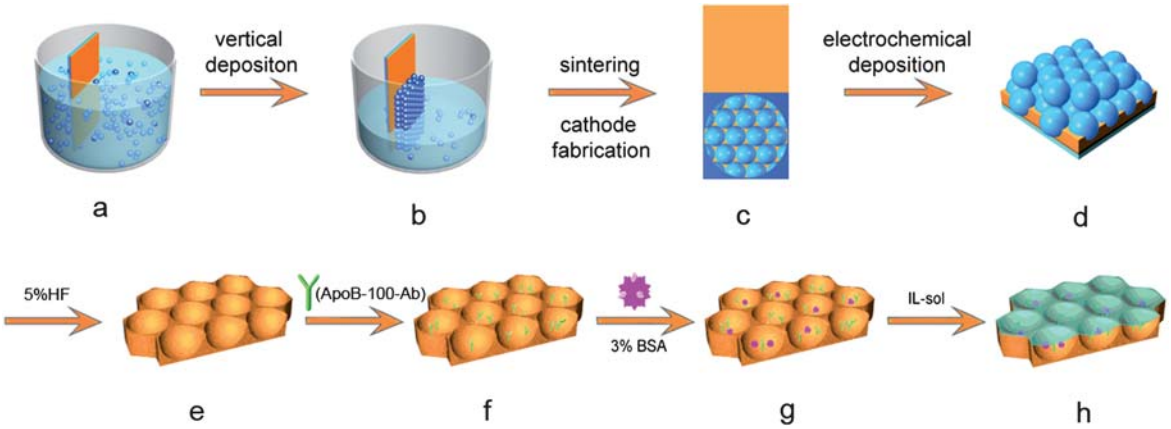

Scheme 1 Schematic Illustration of the Stepwise Immunosensor Fabrication

Ab and BSA molecules firmly in IL-gel membrane (Scheme 1h). The formed ApoB-100 immunosensor was stored at 4 °C when not in use.

2.4 Electrochemical measurements

The prepared ApoB-100 immunosensor was incubated in 400 μL of incubation solution containing different concentrations of ApoB-100 at 60 °C for 40 min and washed carefully with PBS. The EIS measurement was recorded in the frequency range between 0.01 and 1.0×10^5 Hz, at the formal potential of the $[Fe(CN)_6]^{3-/4-}$ redox couple and with a perturbation potential of 5 mV. The CV and EIS measurements were performed in a degassed PBS solution with 0.1M KCl and 2 mM $[Fe(CN)_6]^{3-/4-}$.

The real serum samples were diluted with PBS to the appropriate concentrations from 1 to 10 pg mL^{-1}, respectively. The data of condition optimization and calibration curve were the average of 3 measurements.

3. Results and discussion

3.1 Optimization and characterization of IL-gel membranes

Fig. 1A shows the SEM image of the immunosensor. A wrinkling but uniform IL-gel membrane on the immunosensor was observed, which could effectively prevent protein desorbing from the electrode. On the other hand, the Ab molecules were actually enwrapped by IL in the sol–gel process because of its significant polarity and biocompatibility, which could protect the Ab molecules from being destroyed by ethanol. Moreover, the doping of IL could improve the conductivity of the gel membrane greatly, resulting in the increase of sensitivity. The amount of IL in the IL-gel influences the stability and quality of

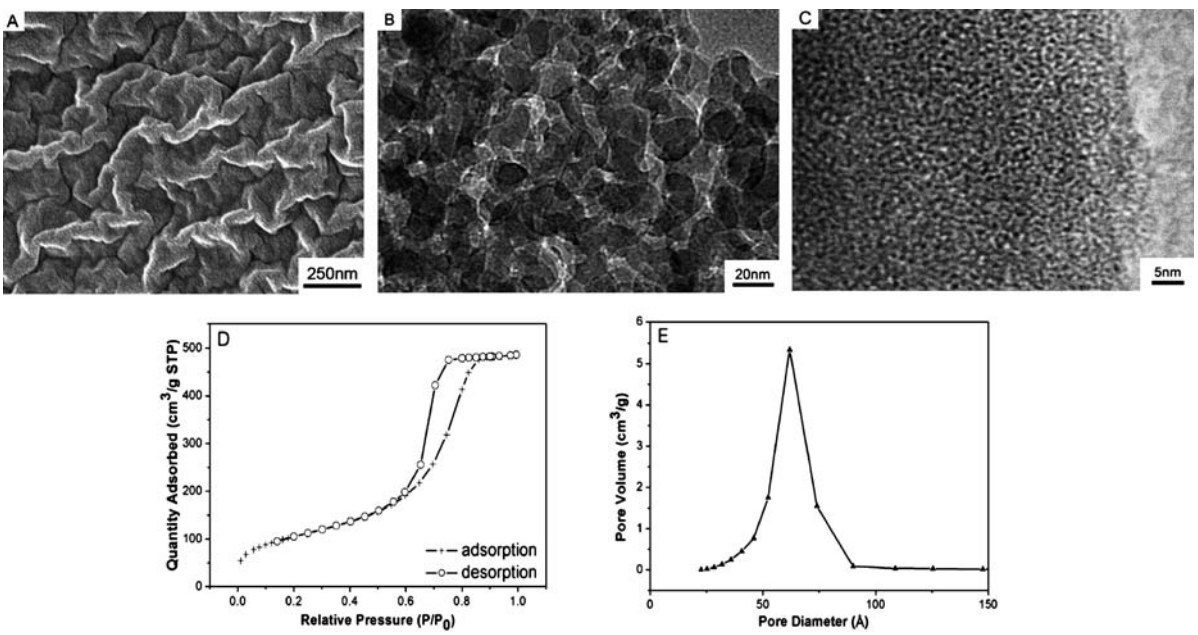

Fig. 1 (A) SEM image of the immunosensor. (B) A representative TEM image of IL-gel sample after calcination at 550 °C. (C) A representative TEM image of pure gel sample after calcination at 550 °C. (D) N_2 adsorption-desorption isotherms of the IL-gel matrix after removal of IL by calcination. (E) The BJH desorption pore size distribution of the IL-gel matrix after removal of IL by calcination.

the complex membrane. Excessive amounts of IL could cause the IL-gel modification unstable because $BMIm^+BF_4^-$ can dissolve in aqueous solution, while deficient amounts of IL can make the membrane crackled because lacking of adhesion of viscous IL. In our experiments, the ratio 2 : 1 (v/v) of TEOS to IL was chosen as the optimization.

Fig. 1B shows a typical TEM image of the porous IL-gel matrix, it exhibited numerous interconnected piled pores around 5 nm, while the pore size of pure gel matrix was less than 1 nm as shown in Fig. 1C. $BMIm^+BF_4^-$ is regarded as a good template for the fabrication of mesoporous silica because of the formation of hydrogen bonds between BF_4^- and silanol group. Obviously, the large pore size of the IL-gel matrix is beneficial to the internal diffusion of probe molecules. The specific surface area and pore volume of the calcined IL-gel matrix were 376.5 $m^2\ g^{-1}$ and 0.75 $cm^3\ g^{-1}$ respectively.

Fig. 1D shows the nitrogen adsorption-desorption isotherms for the calcined IL-gel matrix, it exhibited a hysteresis loop of type H2 in the IUPAC classification, indicating the presence of inter-connection pore network and ink-bottle-like porous structure of the matrix.[40] The pore size distribution was calculated by BJH method as shown in Fig. 1E, and the average diameter of pores was about 5.8 nm. Thus, the bottleneck of the matrix is small enough to prevent the entrapped Ab molecules from leaking out. Moreover, Ab molecules were effectively encapsulated in the host cages of IL-gel matrix, which also prevent protein molecules from unfolding and losing their bioactivities.[41] So the immunosensor exhibited high activity and good thermostability at 60 °C.

In the control experiment, another kind of IL-sol was prepared with $BMIm^+PF_6^-$ and silica sol. However, the conductivity of the IL-gel membrane was greatly decreased for the hydrophobic property of $BMIm^+PF_6^-$. Additionally, once there was no IL doped in the silica sol, a cracked gel membrane could be observed by the naked eye, as a result the immobilized biomolecules were easy to leak out.

3.2 Electrochemical characteristics

Fig. 2A was the CV of ferricyanide which was chosen as a marker to investigate the changes of the electrode behavior after each assembly step. The CV of $[Fe(CN)_6]^{3-/4-}$ at the HOMGF modified electrode is shown as curve a. Adsorption of Ab caused an increase in the peak-to-peak separation of the anodic and cathodic waves and a decrease in the amperometric response (curve b). When BSA was immobilized on the electrode surface, the peak currents decreased greatly (curve c). The reversibility was improved after the covering of IL-gel (curve d), resulting from good conductivity and hydrophilicity of $BMIm^+BF_4^-$. After ApoB-100 was bound with Ab, both of the anodic and cathodic peaks disappeared obviously (curve e) due to the insulation of ApoB-100 molecules. This phenomenon was further confirmed by the results of EIS measurements.

EIS can give more detailed information on the impedance changes in the modification process. The impedance spectrum includes a semicircle portion corresponding to the electron-transfer-limiting process and a linear part resulting from the diffusion-limiting step of the electrochemical process.[42] The diameter of the semicircle exhibits the electron-transfer resistance (R_{et}) of the layer, which controls the electron-transfer kinetics of the redox probe at the electrode interface. Thus, the diameter can be used to describe the interface properties of the electrode.[43] In

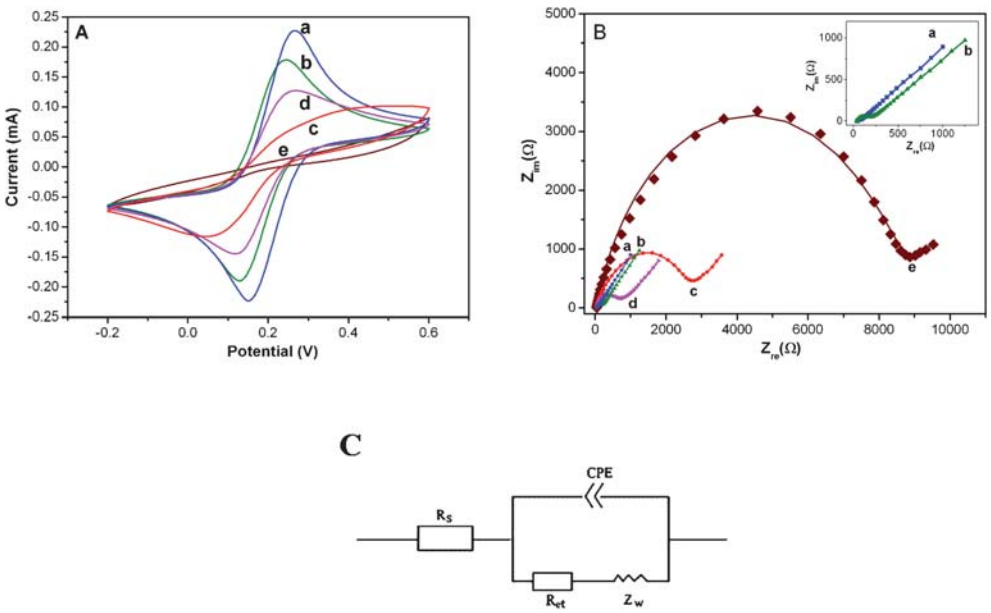

Fig. 2 CVs (A) and EIS (B) of the HOMGF modified electrode with pore size of 250 nm recorded in PBS (50 mM, pH 7.0) solution containing 0.1 M KCl and 2 mM $[Fe(CN)_6]^{3-/4-}$. (a) the HOMGF modified electrode; (b) the Ab/HOMGF modified electrode; (c) the BSA/Ab/HOMGF modified electrode; (d) the IL-gel/BSA/Ab/HOMGF modified electrode; (e) the ApoB-100/IL-gel/BSA/Ab/HOMGF modified electrode. The scan rate of both CV and EIS was 100 mV s^{-1}. The frequency range of EIS is from 0.01 Hz to 100 kHz with signal amplitude of 5 mV. In the Figure B, symbols represented the measured data, while solid lines were the theoretical spectra of equivalent circuits. (C) Equivalent circuit for the impedance spectroscopy in the presence of redox probes using a constant phase element (CPE) instead of capacitance owing to the rough surface.

Fig. 2B, the HOMGF modified electrode reveals a straight line (curve a), implying that the electron-transfer process is not a limiting step of the electrochemical process. Adsorption of the Ab resulted in a small semicircle lying on the Z_{re} axis (curve b), indicating a slight electron-transfer resistance at the electrode interface. The protein layer at the electrode generated a barrier for electron transfer. After saturation of the free active sites of the electrode with BSA, the electron transfer of $[Fe(CN)_6]^{3-/4-}$ was blocked further because of the insulation of BSA (curve c). After the IL-gel membrane was covered on the electrode surface, the impedance value decreased obviously (curve d), and this might be due to the good conductivity of IL which could facilitate the electron transfer between electrode and the probe molecules. Then, R_{et} increased greatly when the sensor was used to detect 5 fg mL^{-1} ApoB-100 (curve e). The isoelectric point of ApoB-100 is 6.58, so it is negatively charged when pH value is 7.0. The electron transfer of $[Fe(CN)_6]^{3-/4-}$ redox couple can be blocked due to the negative charges carried by ApoB-100. Moreover, the ApoB-100 at the electrode also acted as an inert electron and mass-transfer blocking layer. The large active surface area of HOMGF could greatly enhance the amount of adsorbed Ab molecules, which could bind much more ApoB-100 molecules on the electrode surface. Thus, much more obvious differences in EIS could be obtained than in CV responses, showing better sensitivity.

The EIS data can be simulated with an equivalent circuit as shown in Fig. 2C. This equivalent circuit consists of the ohmic resistance of the electrolyte solution (R_s) between the gold working electrode and the SCE reference electrode. The double-layer capacitance (C_{dl}), relating to the surface condition of the electrode. Since the surface of the HOMGF modified electrode was very rough, we use a constant phase element (CPE) instead of the classical capacitance to fit the impedance data.[44–46] Electron-transfer resistance (R_{et}), which exists if a redox probe is present in the electrolyte solution. Warburg impedance (Z_w) resulting from the diffusion of ions from the bulk of the electrolyte to the interface.[47] The two components R_s and Z_w represent the bulk properties of the electrolyte solution and the diffusion of the redox probe in the solution, respectively. Thus, they cannot be affected by chemical transformations at the electrode interface. In our experiments, R_s and Z_w remained nearly unchanged after the modification of the HOMGF. The other two components C_{dl} and R_{et}, depend on the dielectric and insulating features at the electrode/electrolyte interface. Additionally, as can be seen from Fig. 2B, the changes in R_{et} were much larger than other impedance components. Thus, R_{et} was a suitable signal for sensing the interfacial properties of the prepared immunosensor during these assembly procedures.

3.3 Optimization of experimental conditions

The prepared immunosensor was rinsed with PBS and then incubated in an ApoB-100 solution. The ApoB-100 in this solution could be bound to the electrode surface through the specific antigen-antibody reaction between ApoB-100 and Ab, resulting in a change of R_{et}. The change of R_{et} values (ΔR_{et}) after combination with ApoB-100 was calculated by formula $\Delta R_{et} = R_{et(Ab\text{-}Ag)} - R_{et(immunosensor)}$. The effects of incubation temperature and incubation time on the immunoreaction were studied.

The relationship of ΔR_{et} with incubation temperature was studied in a temperature range of 10–80 °C. The fabricated sensor was immersed in a 5 fg mL^{-1} ApoB-100 solution at different temperatures for 60 min. As shown in Fig. 3A, the maximum of ΔR_{et} could be observed amazingly at 60 °C, while white floc was found in a pure Ab aqueous solution at 50 °C which might be due to the inactivation of dissociative Ab molecules. The improved thermal stability of encapsulated Ab could be attributed to reducing the deactivation of the protein molecules in the confined space of the IL-gel host matrix during the thermal treatment process.[45,46,48] It was thought that the hydrogen bond and the electrostatic interaction between IL and protein resulted in a high kinetic barrier for the unfolding of the protein, thus the rigid structure of the protein was protected from being destroyed.[49,50]

Fig. 3B depicts the relationship of ΔR_{et} with incubation time. The immunosensor was immersed in a 5 fg/mL ApoB-100 solution at 60 °C for different time periods. It can be seen that ΔR_{et} increased with the increase of reaction time and then reached a plateau after 40 min. Thus, 40 min of incubation time and 60 °C of incubation temperature were selected for the immunoassay of ApoB-100 combining with the immobilized Ab in the IL-gel membrane.

3.4 Detection of ApoB-100

The pore size of the HOMGF modified electrode plays an important role on the sensitivity of immunoreaction. In the case

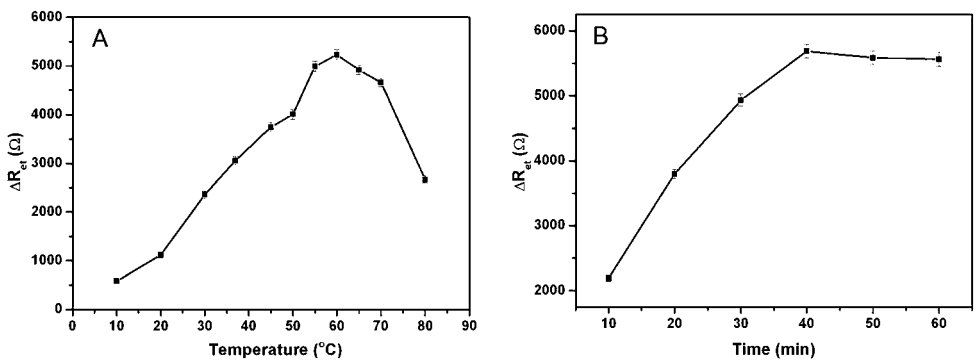

Fig. 3 Relationship of ΔR_{et} with the incubation temperature (A) and incubation time (B) on the response of EIS.

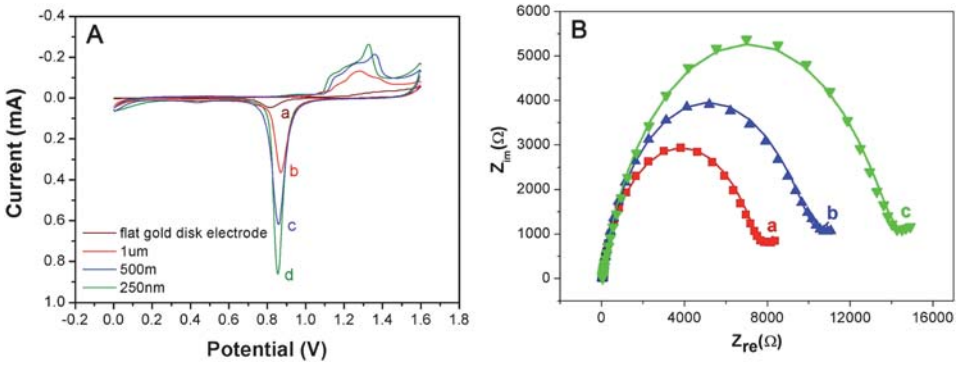

Fig. 4 (A) CVs of the HOMGF modified electrodes with different diameters of template SiO_2 particles in 0.5 M H_2SO_4 at a scan rate of 100 mV s^{-1} (curves b–d). For comparison, the CV of a flat gold disk electrode is also shown (curve a). (B) Impedance responses to the same concentration of ApoB-100 PBS solution on the HOMGF modified electrodes with different diameter of the template SiO_2 particles of 1 μm (curve a), 500 nm (curve b) and 250 nm (curve c). Faradaic impedance spectra were recorded in PBS (50mM, pH 7.0) solution containing 0.1 M KCl and 2mM $[Fe(CN)_6]^{3-/4-}$. In this Figure, symbols represented the measured data, while solid lines were the theoretical spectra of equivalent circuits.

of the CV characterization of HOMGF modified electrodes depicted in Fig. 4A, the active surface area of HOMGF modified electrode with template SiO_2 particles of 250 nm was the largest. Fig. 4B shows the impedance responses of the ApoB-100 immunosensors with different HOMGFs in a PBS solution containing 0.5 pg/mL of ApoB-100. The diameter of the template SiO_2 particles of these HOMGFs are 1μm (curve a); 500 nm (curve b) and 250 nm (curve c) respectively. The impedance value of curve c was bigger than that of curve b or curve a. The larger was the electrode surface area, the more amount of Ab can be immobilized, and thus the bigger ΔR_{et} may be observed by combination of ApoB-100 molecules.

To evaluate the inter-reaction between Ab and ApoB-100, the immunosensor was exposed into various concentrations of ApoB-100 solutions, C_{Ag}. Before EIS measurements were performed, CV was carried out until the currents did not change anymore. The corresponding Nyquist plots of impedance spectra are shown in Fig. 5A. The interfacial electron-transfer resistances increased proportionally with the concentrations of ApoB-100 in PBS solution, implying that when a higher concentration of ApoB-100 bound to the immobilized Ab molecules, it would generate a denser blocking layer to the electron transfer of the redox probe. The linear relationship between the ΔR_{et} and the logarithm of the ApoB-100 concentrations was obtained from 5 fg mL^{-1} to 50 pg/mL with a correlation coefficient of 0.98 (Fig. 5B). As can be seen, ΔR_{et} increased with increasing ApoB-100 concentrations within the detection range. However, the increases in ΔR_{et} were not obvious at higher ApoB-100 concentrations due to steric hindrance or saturation of coupled antigen molecules. According to the linear equation, we could detect ApoB-100 concentrations quantitatively.

In the control experiment, $BMIm^+PF_6^-$ was used as additive in the IL-gel membrane to immobilize Ab and BSA. Then, the sensor was used to detect various concentrations of ApoB-100, the Nyquist plots of impedance spectra are shown in Fig. 6. The impedance value of $BMIm^+PF_6^-$-gel modified electrode is extraordinary large, up to about 13 000 Ω (curve a), while that of $BMIm^+BF_4^-$-gel modified electrode is only 682 Ω. The poor conductivity of $BMIm^+PF_6^-$-gel membrane is probably the hydrophobic nature of $BMIm^+PF_6^-$, thus the electron transfer between redox probe of $[Fe(CN)_6]^{3-/4-}$ and electrode surface could be inhibited.[51] The interfacial R_{et} of the immunosensor is so high that the response nearly does not change with the increase of ApoB-100 concentration (curve b to f).

To verify the hydrophilicity or hydrophobicity for IL, the wetting properties of the materials were investigated by

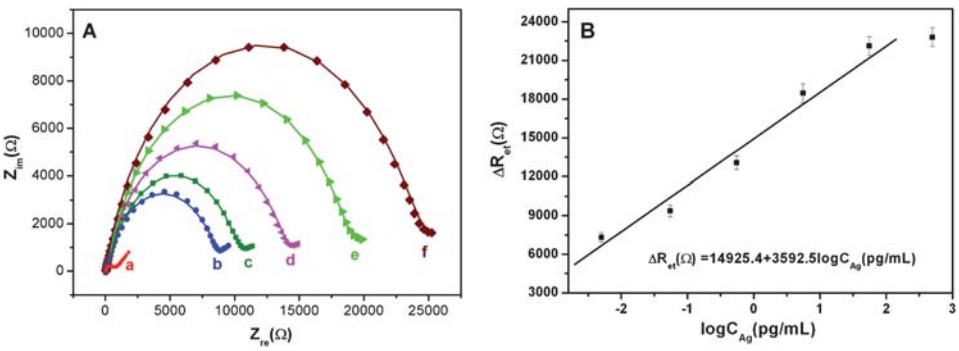

Fig. 5 (A) Faradaic impedance spectra that corresponded to the fabricated immunosensor at 60 °C, before and after incubating with different concentrations of ApoB-100 in PBS (20 mM, pH 7.0) solution containing 0.1 M KCl and 5 mM $Fe(CN)_6^{3-/4-}$: (a) blank solution; curves b–f represent 0.005, 0.05, 0.5, 5.0 and 50.0 pg/mL ApoB-100, respectively. (B) Calibration curve for the ApoB-100 immunosensor. In the Fig. 6A, symbols represented the measured data, while solid lines were the theoretical spectra of equivalent circuits.

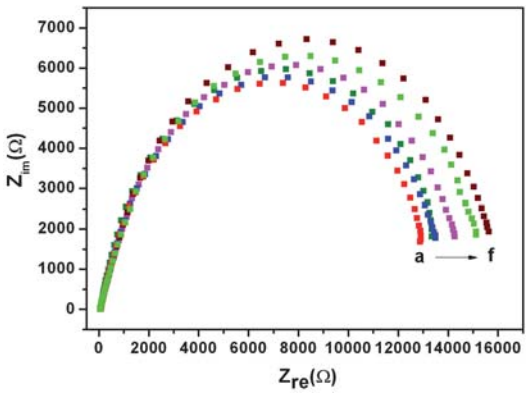

Fig. 6 Faradaic impedance spectra corresponding to the control experiment with $BMIm^+PF_6^-$ used as additive in IL-gel membrane, before and after incubating with different concentrations of ApoB-100 in PBS (20 mM, pH 7.0) solution containing 0.1 M KCl and 5 mM $Fe(CN)_6^{3-/4-}$: (a) blank solution; curves b–f represent 0.005, 0.05, 0.5, 5.0 and 50.0 pg/mL ApoB-100, respectively.

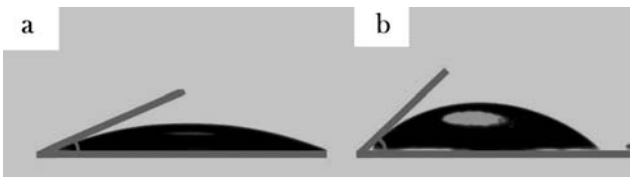

Fig. 7 Contact angels of water on: (a) HOMGF/Ab-BSA/BMIm + BF_4^--gel membrane and (b) HOMGF/Ab-BSA/BMIm + PF_6^--gel membrane.

measuring the water contact angles (θ) on the surface of HOMGF/Ab-BSA/IL-gel modified electrodes. The result could be observed in Fig. 7, the contact angles of water on HOMGF/Ab-BSA/$BMIm^+BF_4^-$-gel membrane (a) and HOMGF/Ab-BSA/$BMIm^+PF_6^-$-gel membrane (b) were detected as 28° and 45° respectively, showing that $BMIm^+PF_6^-$ is much more hydrophobic than $BMIm^+BF_4^-$.

3.5 Nonspecific interactions

Usually, nonspecific adsorption is a major problem in label-free immunosensing, since it cannot be distinguished from specific adsorption in unlabeled electrochemical sensing antigens. Nonspecific interaction test between the fabricated ApoB-100 sensor and other protein with different concentrations was performed. Fig. 8 shows calibration plots that correspond to the ΔR_{et} caused by different concentrations of target analyte (ApoB-100) and contrast analyte (PAB). PAB is a reliable index of liver function. As can be seen in Fig. 8, there is only a slight variation on the impedance with the increase of PAB. Such small ΔR_{et} of the nonspecific Ab molecules adsorption are acceptable. Thus, the immunosensor is feasible for the determination of ApoB-100 in serum.

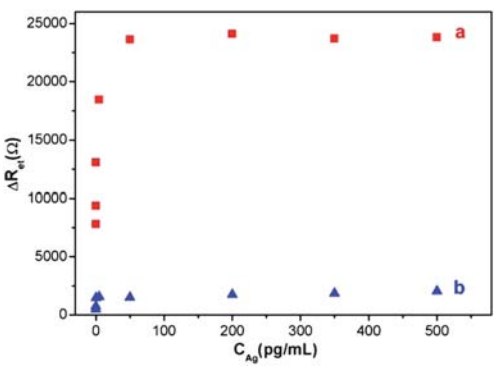

Fig. 8 The concentrations of (a) ApoB-100 and (b) PAB *via* ΔR_{et} for the immunosensor.

3.6 Stability, reproducibility, and regeneration of the immunosensor

When the sensor was stored at 4 °C over 40 days, no apparent change in the same ApoB-100 concentration was found, indicating that the immunosensor had good stability. The reproducibility of the sensor was estimated with intra- and inter-assay precision. The intra-assay precision was evaluated by assaying one ApoB-100 level for three replicate measurements. The inter-assay precision was estimated by determining one ApoB-100 level with three immunosensors made at the same experimental conditions. The intra- and inter-assay variation coefficients (CVs) obtained from 10 pg/mL ApoB-100 were 5.3% and 6.7%, respectively. Obviously, the inter-assay CV showed a good electrode-to-electrode reproducibility of the fabrication protocol, while the low value of intra-assay CV indicated that the immunosensor could be regenerated and used repeatedly.

Regeneration of the immunosensor is of interest to immunoassay. In the experiment, 0.2 M glycine-hydrocholric acid (Gly-HCl) buffer solution (pH 2.8) was chosen to break the antibody-antigen linkage. After detecting ApoB-100, the sensor was dipped into Gly-HCl buffer solution for 10 min to remove ApoB-100 from Ab. The as-renewed immunosensor could restore 95% of the initial signal after three assay runs, showing good reusability and stability. In addition, after three assay cycles, if the immunosensor was treated first with 20% (w/w) NaOH to remove rigid IL-gel membrane and then with piranha solution to violently peel all adsorbed biomolecules from the HOMGF surface, complete renewal of the modified electrode could be achieved, with the reuse lifetime of more than 10 times.

3.7 Application of the immunosensor in human ApoB-100 levels

The ApoB-100 levels in five serum samples were obtained using the proposed immunosensor as shown in Table 1, and were compared with the immunonephelometry technology performed in Affiliated Drum Tower Hospital of Nanjing University Medical School for clinical diagnosis. There is no significant difference between the results and the traditional clinical method.

Table 1 Comparison of ApoB-100 Determinations on Human Serum Samples by the proposed immunosensor and immunonephelometry

Serum samples	1	2	3	4	5
Our method/pg mL^{-1}	5.6	1.8	7.8	1.3	4.6
immunonephelometry/pg mL^{-1}	5.9	1.7	8.0	1.2	4.8
Relative deviation (%)	−5.1	+5.9	−2.5	+8.3	−4.2

Thus, the developed versatile immunoassay may provide a satisfactory alternative tool for the clinical determination of ApoB-100 levels in human serum.

4. Conclusion

The EIS response of the fabricated ApoB-100 immunosensor could be greatly enhanced by immobilizing Ab molecules in IL-gel composite membrane on a HOMGF modified electrode. The high sensitivity of the immunosensor was mainly contributed to the excellent biocompatibility, stability and conductivity of IL, as well as the large active surface area of HOMGF. The developed immunosensor has also been successfully applied to the detection of ApoB-100 in real human serum samples, and this might open new avenues to apply ILs in immunoassays.

Acknowledgements

We greatly appreciate the support from the National Natural Science Foundation of China for Key Program (20635020), General Program (20905035, 20805030) and Creative Research Group (20821063). This work is also supported by National Basic Research Program of China (2006CB933201). We also thank Professor Kui Zhang from The Affilizted Drum Tower Hospital of Nanjing University Medical School, Nanjing University for her kind help.

Notes and references

1 T. O. Cheng, *Chin. Med. J.*, 2005, **118**, 355.
2 A. J. Lusis, *Nature*, 2000, **407**, 233.
3 M. Haidaria, M. Moghadamb, M. Chinicarb, A. Ahmadiehb and M. Doostic, *Clin. Biochem.*, 2001, **34**, 149.
4 C. A. Dane-Stewart, G. F. Watts, J. C. L. Mamo, S. B. Dimmittm, P. H. R. Barrett and T. G. Redgrave, *Eur. J. Clin. Invest.*, 2001, **31**, 113.
5 X. Y. Wang, R. Pease, J. Bertinato and R. W. Milne, *Arterioscl. Throm. Vas.*, 2000, **20**, 1301.
6 K. Miyoshi, E. Uchida and M. J. Niiyama, *J. Vet. Med. Sci.*, 2000, **62**, 1269.
7 Y. Y. Lin, J. Wang, G. D. Liu, H. Wu, C. M. Wai and Y. H. Lin, *Biosens. Bioelectron.*, 2008, **23**, 1659.
8 C. L. Hong, R. Yuan, Y. Q. Chai and Y. Zhuo, *Electroanalysis*, 2008, **20**, 989.
9 G. F. Jie, H. P. Huang, X. L. Sun and J. J. Zhu, *Biosens. Bioelectron.*, 2008, **23**, 1896.
10 G. F. Jie, B. Liu, H. C. Pan, J. J. Zhu and H. Y. Chen, *Anal. Chem.*, 2007, **79**, 5574.
11 W. Yan, X. J. Chen, X. H. Li, X. M. Feng and J. J. Zhu, *J. Phys. Chem. B*, 2008, **112**, 1275.
12 H. Chen, J. H. Jiang, Y. Huang, T. Deng, J. S. Li, G. L. Shen and R. Q. Yu, *Sens. Actuators, B*, 2006, **117**, 211.
13 C. Ji and P. C. Searson, *J. Phys. Chem. B*, 2003, **107**, 4494.
14 N. Miura, K. Ogata, G. Sakai, T. Uda and N. Yamazoe, *Chem. Lett.*, 1997, 713.
15 D. R. Shankaran, K. V. Gobi, T. Sakai, K. Matsumoto, K. Toko and N. Miura, *Biosens. Bioelectron.*, 2005, **20**, 1750.
16 S. M. Renaud, D. Dupont and P. Dulieu, *J. Agric. Food Chem.*, 2004, **52**, 659.
17 M. Hendrix, E. S. Priestley, G. F. Joyce and C. H. Wong, *J. Am. Chem. Soc.*, 1997, **119**, 3641.
18 W. Senaratne, L. Andruzzi and C. K. Ober, *Biomacromolecules*, 2005, **6**, 2427.
19 F. Frederix, K. Bonroy, W. Laureyn, G. Reekmans, A. Campitelli, W. Dehaen and G. Maes, *Langmuir*, 2003, **19**, 4351.
20 K. V. Gobi, C. Kataoka and N. Miura, *Sens. Actuators, B*, 2005, **108**, 784.
21 K. Kato, C. M. Dooling, K. Shinbo, T. H. Richardson, F. Kaneko, R. Tregonning, M. O. Vysotsky and C. A. Hunter, *Colloids Surf., A*, 2002, **198–200**, 811.
22 F. Davis and S. P. J. Higson, *Biosens. Bioelectron.*, 2005, **21**, 1.
23 K. S. Phillips, J. H. Han, M. Martinez, Z. Wang, D. Carter and Q. Cheng, *Anal. Chem.*, 2006, **78**, 596.
24 A. Bossi, F. Bonini, A. P. F. Turner and S. A. Piletsky, *Biosens. Bioelectron.*, 2007, **22**, 1131.
25 M. A. Cooper, A. C. Try, J. Carroll, D. J. Ellar and D. H. Williams, *Biochim. Biophys. Acta, Biomembr.*, 1998, **1373**, 101.
26 D. Avnir, T. Coradin, O. Lev and J. Livage, *J. Mater. Chem.*, 2006, **16**, 1013.
27 E. H. Lan, B. Dunn and J. I. Zink, *Chem. Mater.*, 2000, **12**, 1874.
28 M. T. Reetz, A. Zonta and J. Simpelkamp, *Angew. Chem., Int. Ed. Engl.*, 1995, **34**, 301.
29 P. Vidinha, V. Augusto, M. Almeida, I. Fonseca, A. Fidalgo, L. Ilharco, J. M. S. Cabral and S. Barreiros, *J. Biotechnol.*, 2006, **121**, 23.
30 A. C. Pierre, *Biocatal. Biotransform.*, 2004, **22**, 145.
31 M. T. Reetz, P. Tielmann, W. Wiesenhöfer, W. Könen and A. Zonta, *Adv. Synth. Catal.*, 2003, **345**, 717.
32 F. Péter, L. Poppe, C. Kiss, E. Szoc-Bíró, G. Preda, C. Zarcula and A. Olteanu, *Biocatal. Biotransform.*, 2005, **23**, 251.
33 J. D. Brennan, D. Benjamin, E. DiBattista and M. D. Gulcev, *Chem. Mater.*, 2003, **15**, 737.
34 J. L. Anderson, D. W. Armstrong and G. T. Wei, *Anal. Chem.*, 2006, **78**, 2892.
35 Y. Liu, M. J. Wang, J. Li, Z. Y. Li, P. He, H. T. Liu and J. H. Li, *Chem. Commun.*, 2005, 1778.
36 S. H. Lee, T. T. N. Doan, S. H. Ha, W. J. Chang and Y. M. Koo, *J. Mol. Catal. B: Enzym.*, 2007, **47**, 129.
37 G. C. Zhao, M. Q. Xu, J. Ma and X. W. Wei, *Electrochem. Commun.*, 2007, **9**, 920.
38 X. H. Li, L. Dai, Y. Liu, X. Chen, W. Yan, L. L. Jiang and J. J. Zhu, *Adv. Funct. Mater.*, 2009, **19**, 3120.
39 X. J. Chen, Y. Y. Wang, J. J. Zhou, W. Yan, X. H. Li and J. J. Zhu, *Anal. Chem.*, 2008, **80**, 2133.
40 Y. Han, S. S. Lee and J. Y. Ying, *Chem. Mater.*, 2006, **18**, 643.
41 Y. Wei, J. Xu, Q. Feng, M. Lin, H. Dong, W. Zhang and C. Wang, *J. Nanosci. Nanotechnol.*, 2001, **1**, 83.
42 H. Chen, J. J. Jiang, Y. Huang, T. Deng, J. S. Li, G. L. Shen and R. Q. Yu, *Sens. Actuators, B*, 2006, **117**, 211.
43 S. Hleli, C. Martelet, A. Abdelghani, F. Bessueile, A. Errachid, J. Samitier, H. C. W. Hays, P. A. Millner, N. Burais and N. Jaffrezic-Renault, *Mater. Sci. Eng., C*, 2006, **26**, 322.
44 T. J. Pajkossy, *J. Electroanal. Chem.*, 1994, **364**, 111.
45 R. De Levie, *Electrochim. Acta*, 1965, **10**, 113.
46 W. Scheider, *J. Phys. Chem.*, 1975, **79**, 127.
47 E. Katz and I. Willner, *Electroanalysis*, 2003, **15**, 913.
48 H. Pfruender, M. A. U. Kragl and D. Weuster-Botz, *Angew. Chem., Int. Ed.*, 2004, **43**, 4529.
49 C. Lei, Y. Shin, J. Liu and E. J. Ackerman, *J. Am. Chem. Soc.*, 2002, **124**, 11242.
50 Y. J. Han, G. D. Stucky and A. Bulter, *J. Am. Chem. Soc.*, 1999, **121**, 9897.
51 S. Rivera-Rubero and S. Baldelli, *J. Am. Chem. Soc.*, 2004, **126**, 11788.

